

Available online at www.sciencedirect.com

ScienceDirect

journal homepage: www.elsevier.com/locate/yexcr

Research Article

Context dependent reversion of tumor phenotype by connexin-43 expression in MDA-MB231 cells and MCF-7 cells: Role of β -catenin/connexin43 association



Rabih S. Talhouk^{a,*}, Mohamed-Bilal Fares^{a,1}, Gilbert J. Rahme^{a,2}, Hanaa H. Hariri^{a,3}, Tina Rayess^{a,4}, Hashem A. Dbouk^{a,5}, Dana Bazzoun^a, Dania Al-Labban^{a,6}, Marwan E. El-Sabban^{b,**}

^aDepartment of Biology, Faculty of Arts and Sciences, American University of Beirut, P.O. Box 11-0236, Beirut, Lebanon

^bDepartment of Anatomy, Cell Biology and Physiology, Faculty of Medicine, American University of Beirut, P.O. Box 11-0236, Beirut, Lebanon

ARTICLE INFORMATION

Article Chronology:

Received 27 December 2012

Received in revised form

10 September 2013

Accepted 1 October 2013

Available online 10 October 2013

Keywords:

Gap junction intercellular communication

Connexin

Breast Cancer

Catenin

ABSTRACT

Connexins (Cx), gap junction (GJ) proteins, are regarded as tumor suppressors, and Cx43 expression is often down regulated in breast tumors. We assessed the effect of Cx43 over-expression in 2D and 3D cultures of two breast adenocarcinoma cell lines: MCF-7 and MDA-MB-231. While Cx43 over-expression decreased proliferation of 2D and 3D cultures of MCF-7 by 56% and 80% respectively, MDA-MB-231 growth was not altered in 2D cultures, but exhibited 35% reduction in 3D cultures. C-terminus truncated Cx43 did not alter proliferation. Untransfected MCF-7 cells formed spherical aggregates in 3D cultures, and MDA-MB-231 cells formed stellar aggregates. However, MCF-7 cells over-expressing Cx43 formed smaller sized clusters and Cx43 expressing MDA-MB-231 cells lost their stellar morphology. Extravasation ability of both MCF-7 and MDA-MB-231 cells was reduced by 60% and 30% respectively. On the other hand, silencing Cx43 in MCF10A cells, nonneoplastic human mammary cell line, increased proliferation in both 2D and 3D cultures, and disrupted acinar morphology. Although Cx43 over-expression did not affect total levels of β -catenin, α -catenin and ZO-2, it decreased nuclear levels of β -catenin in 2D and 3D cultures of MCF-7 cells, and in 3D cultures of MDA-MB-231 cells. Cx43 associated at the membrane with α -catenin, β -catenin and ZO-2 in 2D and 3D cultures of MCF-7 cells, and only in

*Corresponding author. Fax: +961 1 374374x3888.

**Corresponding author. Fax: +961 1 744 464.

E-mail addresses: rtalhouk@aub.edu.lb (R.S. Talhouk), me00@aub.edu.lb (M.E. El-Sabban).

¹ Present address: Brain Mind Institute, School of Life Sciences, Ecole Polytechnique Fédérale de Lausanne (EPFL), Lausanne CH-1015, Switzerland.

² Present address: Genetics Department, Norris Cotton Cancer Center, Dartmouth Medical School program, Dartmouth College, New Hampshire, 03755, U.S.A.

³ Present address: Institute of Molecular Biophysics, Florida State University, Tallahassee, FL 32306, USA.

⁴ Present address: Department of Cardiothoracic Surgery, Department of Cell and Developmental Biology, Weill Cornell Medical College and the Weill Graduate School of Medical Sciences of Cornell University New York, NY 10065, USA.

⁵ Present address: Department of Pharmacology, UT Southwestern Medical Center, Dallas, TX 75390, USA.

⁶ Present address: Department of Biochemistry, University of Lausanne, 1015 Lausanne, Switzerland.

3D conditions in MDA-MB-231 cells. This study suggests that Cx43 exerts tumor suppressive effects in a context-dependent manner where GJ assembly with α -catenin, β -catenin and ZO-2 may be implicated in reducing growth rate, invasiveness, and, malignant phenotype of 2D and 3D cultures of MCF-7 cells, and 3D cultures of MDA-MB-231 cells, by sequestering β -catenin away from nucleus.

© 2013 Elsevier Inc. All rights reserved.

Introduction

Direct cell–cell interaction is mediated by a variety of junctional complexes that maintain proper tissue homeostasis. Adherens junctions, tight junctions, and gap junctions (GJs) play overlapping roles in the development and differentiation of many tissues, and the disruption of any of them has been associated with various diseases, including cancer [1,2]. For instance, it has been shown that GJs, the main junctions that permit the transfer of small molecules between cells via GJIC, are downregulated during primary tumor initiation [3–5]. Moreover, it has been established that while the re-expression of different connexin (Cx) proteins (the building blocks of GJs) into tumor cells decreases their growth rates and inhibits their invasive abilities [6–9], Cx down-regulation increases tumor cell malignancy [10]. It is assumed that cancerous cells at the primary tumor site tend to downregulate Cxs simply in order to inhibit the assembly of GJs so as to release themselves from their physical constraints, hence allowing easier proliferation and free cell movement. Interestingly, the mechanisms mediating the tumor suppressive effects of Cxs remain largely unknown, and have been shown to be mediated independently of GJIC [11].

Nevertheless, several studies have illustrated the importance of GJ assembly and GJIC in development, in maintenance of tissue homeostasis, and in differentiation of various tissues [12–14], including the mammary gland [15]. In fact, studies from our lab have shown that Cxs are highly regulated during mammary gland development and differentiation [16], and that mammary epithelial cell differentiation in vitro relies on GJIC in a β 1-integrin independent and possibly OCT-1 dependent manner [17,18]. Moreover, we have shown that under conditions favoring mammary epithelial differentiation, β -catenin (which is a key player of the Wnt signaling pathway) is sequestered by GJ complexes at the membrane, away from the nucleus [19] where it usually promotes cellular proliferation, angiogenesis, invasion, motility, differentiation and stem cell renewal [20]. Given that the fundamental processes required for mammary gland development and differentiation are usually deregulated in breast cancers [21,22], we propose that the tumor-suppressive role played by Cxs is indeed independent of GJIC and the transfer of small molecules between cells, but is mediated via Cx-associated proteins within the GJ complex, in a mechanism that involves sequestering β -catenin at the membrane. In some breast cancer cell lines, Cx overexpression was only successful in reverting the tumorigenic phenotype when cells were cultured in conditions mimicking the original micro-environment, i.e. on Engelbreth-Holm Swarm (EHS) reconstituted basement membrane [23], or when cells were implanted into the mammary fat pads of nude mice [5]. These studies suggest that the tumor suppressive effect of Cx over-expression is conveyed in a context-dependent manner that perhaps allows the proposed assembly of GJ complexes.

This study aims to address the mechanism via which Cx43 mediates its tumor suppressive effects, and investigate the possible role for GJ complex assembly in 2D and 3D cultures of low invasive MCF-7 and highly invasive MDA-MB-231 breast cancer cells, with primary emphasis on the role played by β -catenin and other Cx-associated partners. The two cell lines were stably transfected with Cx43 and the effect of Cx43 over-expression on the morphology and proliferation in 2D and 3D growth conditions in addition to their trans-endothelial migration potential was assessed. We also studied changes in Cx-associated proteins, in particular β -catenin, and whether these may be implicated in any of the observed effects. Our results suggest that reversion of a tumor phenotype is context dependent and associates with Cx43 assembly into GJ complexes at the membrane of breast cancer cells, and the recruitment of β -catenin from the nucleus into such complexes.

Materials and methods

Cell culture

MCF-7 and MDA-MB-231, human mammary adenocarcinoma cell lines, and MCF10A, nonneoplastic human mammary cell line, kindly provided by Dr. Mina Bissell (LBNL, CA), were grown in humidified incubator (95% air, 5% CO₂) at 37 °C. MCF-7 and MDA-MB-231 cells were cultured in RPMI 1640 medium with 10% Fetal Bovine Serum (FBS) (Sigma, St. Louis) and MCF10A cells in DMEM F-12 medium (Lonza, Belgium) supplemented with 5% horse serum, 20 ng/ml EGF, 0.5 μ g/ml hydrocortisone, 100 ng/ml cholera toxin, and 10 μ g/ml insulin. All media were supplemented with 1% penicillin–streptomycin. When reaching 80% confluence, cells were washed with 1 \times Dulbecco's Phosphate Buffered Saline (PBS) then incubated with 2 \times trypsin (containing 5.0 g porcine trypsin, 2.0 g EDTA, 4NA per liter of 0.9% NaCl; Sigma, St. Louis) at 37 °C for 1 min. For three-dimensional cultures, Growth Factor Reduced Matrigel obtained from BD Biosciences was used. 35 mm culture dishes were coated with 500 μ l of growth factor-reduced Matrigel, and then incubated at 37 °C for 30 min to form a bed of 100% solidified EHS measuring approximately 1–2 mm in thickness. Cells were diluted in complete media with 2% EHS, to achieve a final concentration of 50,000 cells/ml. Cells were supplemented with fresh complete media with 2% EHS every two days. Clusters start to form by day 3, and cells were kept in culture for 8 days.

pEGFP-N1 and pGFP-V-RS plasmid vectors

pEGFP-N1: for Cx43 overexpression, total RNA from MCF-7 cells was extracted using TRIZOL reagent (Invitrogen), then treated with DNase I (Amersham Pharmacia Biotech). RT-PCR was then

used to produce a cDNA covering the complete reading frame of mouse Cx43 and another that codes for a C-terminus truncated version of Cx43 having the complete sequence up to amino acid 242. The cDNAs were inserted downstream of a cytomegalovirus promoter (CMV) to the amino terminus of Enhanced Green fluorescent Protein (EGFP) (Clontech).

pGFP-V-RS: for Cx43 silencing, four unique constructs against Cx43 (shRNA-Cx43), one construct containing non-effective scrambled Cx43 (shRNA-scr), and one construct lacking the shRNA insert were purchased from OriGene Technologies, Inc.

The above vectors were purified and cloned into QIAGEN PCR Cloning kit (Qiagen) using pDrive Cloning vector. Then they were transformed into DH5 α competent bacteria by heat shock and plasmids were purified using midi plasmid purification kit (Qiagen). Adequate restriction digestion enzymes were used to verify the purified plasmids before amplification.

Transfection

MDA-MB-231, MCF-7 and MCF10A cells were plated on 35 mm diameter tissue culture plates, at a density of 0.5×10^6 cells/well in 2 ml of media. After 24 h, media was removed, and cells were first washed with $1 \times$ PBS then washed with OptiMEM media (Gibco, UK). Transfection was performed using Lipofectamine-Plus reagent (Invitrogen), according to manufacturer's instructions. Selection of MCF-7 and MDA-MB-231 transfected cells was in RPMI with 1% penicillin-streptomycin (Gibco, UK) and 10% FBS supplemented with 400 μ g/ml and 600 μ g/ml geneticin (Gibco, UK) for MCF-7 and MDA-MB-231 respectively. 0.35 μ g/ml puromycin was used to select for transfected MCF10A cells. Selection medium was used throughout the study.

Protein extraction and immunoblotting

Total cellular protein extraction

For two-dimensional cultures, cells used for protein extraction are collected at 80% confluency. Cells were scraped into 300 μ l of lysis buffer (50 mM Tris-Cl, pH 7.5, 150 mM NaCl, 1% Nonidet P40, 0.5% Sodium deoxycholate) to which 40 μ l/ml Protease inhibitors (CompleteTM) and 40 μ l/ml phosphatase inhibitors were added. DC Protein Assay (Bio-Rad, Hercules, CA) was used to quantify proteins using bovine serum albumin (BSA, Sigma Chemical Co.) as standards. For three-dimensional cultures, cells were dissociated using PBS-EDTA (2.5 mM) followed by collection of cell pellets and addition of 150 μ l lysis buffer to the cell pellet.

Extraction of nuclear proteins

Cells are gently scraped with $1 \text{ ml } 1 \times$ PBS (Lonza, Belgium) into a microcentrifuge tube and centrifuged at $1000 \times g$ for 10 min at 4 $^{\circ}\text{C}$ to obtain a cell pellet. The pellet is lysed by rapid freezing and thawing and then resuspended into 70 μ l of hypotonic Buffer A (10 mM Hepes pH 7.9, 10 mM KCl, 1.5 mM MgCl₂, and 1 mM Dithiothreitol), incubated for 10 min at 4 $^{\circ}\text{C}$, and then vortexed for 10 s. The mixture was centrifuged at $4500 \times g$ for 10 min, and the pellet (representing nuclei) was resuspended in 15 μ l of hypertonic Buffer C (20 mM Hepes pH 7.9, 0.4 M NaCl, 1.5 mM MgCl₂, 25% (v/v) Glycerol, 0.2 mM EDTA, 1 mM Dithiothreitol, 0.5 mM PMSF), placed on a shaker for 30 min at 4 $^{\circ}\text{C}$, and then centrifuged at $14,000 \times g$ for 20 min. The supernatant is diluted with 30 μ l of Diluting Buffer D (20 mM Hepes, 50 mM KCl, 20% (v/v) Glycerol,

0.2 mM EDTA, 1 mM Dithiothreitol, 0.5 mM PMSF) and stored at -20°C .

Western blot analysis of proteins

On basis of equal protein loading, protein extracts were resolved on polyacrylamide gels. After electrophoresis, proteins were transferred overnight on the immobilin blot polyvinylidene difluoride (PVDF) membrane (BioRad, Hercules, CA) using wet blot apparatus in transfer buffer (39 mM glycine, 48 mM Tris base, 0.037% SDS and 20% methanol). Blocking of the membranes was carried out for 1.5–2 h in wash buffer (100 mM Tris-Cl, pH 8, 150 mM NaCl, 0.1% Tween-20) with 5% skimmed milk, then incubated overnight at 4 $^{\circ}\text{C}$ with 1% milk in wash buffer with the primary antibody, of interest (dilutions were typically 1:400 unless specified otherwise by company's datasheet). The bound antibody was detected by addition of the corresponding horse reddish peroxidase conjugated IgG (Santa Cruz Biotechnology, Santa Cruz, CA) followed by enhanced chemiluminescence (ECL, Santa Cruz). All incubations were performed at room temperature. Equal loading was determined by probing total extracts for mouse anti-GAPDH (1:10000-v/v) and probing nuclear extracts for Lamin A/C (1:5000-v/v).

Quantitative analysis of nuclear β -catenin Western blots

NIH Image 1.62 software was used for densitometric quantitation of Western blots for nuclear β -catenin. Quantification was normalized in reference to the Lamin A/C. ANOVA uni-variant test using the Graph Pad Prism software version 3.00 was used for statistical significance. Quantifications were from three different experiments.

Quantitative real time PCR (qRT-PCR)

Total RNA was extracted from cells using RNeasy Minikit (Qiagen) according to the manufacturer's instructions. 1 μ g of total RNA was reversed transcribed to cDNA using Revertaid 1st strand cDNA synthesis kit (Fermentas). RT-PCR was performed using iQ SYBR Green Supermix in a CFX96 system (Bio-Rad Laboratories). Products were amplified using primers for Cx43: 5'-CAAATCGAATGGGG-CAGGC-3' (forward) and 5'-GCTGGTCCAAATGGCTAGT-3' (reverse), and for GAPDH: 5'-AAGGTGAAGGTCCGAGTCAAC-3' (forward) and 5'-GGGGTCATTGATGGCAACAATA-3' (reverse). To quantify changes in gene expression, the comparative C_t method was used to calculate the relative-fold changes normalized to GAPDH.

Co-immunoprecipitation

Cell pellets resulting from 2D or 3D cultures were suspended in RIPA buffer (50 mM Tris-Cl, pH 7.5, 150 mM NaCl, 1% Nonidet P40, 0.5% Sodium deoxycholate and 0.1% SDS) supplemented with Protease inhibitors (CompleteTM) at a concentration of 10 μ l/ml and phosphatase inhibitors at a concentration of 40 μ l/ml. Cell extracts were centrifuged at $14,000 \times g$ for 30 min. The supernatants were collected and precleared with protein A agarose beads (Roche Applied Science) and incubated at 4 $^{\circ}\text{C}$ for 1 h. Protein A agarose beads were collected by centrifugation at $14,000 \times g$ at 4 $^{\circ}\text{C}$ for 10 min, supernatants were removed and incubated with 1 μ g of primary antibody at 4 $^{\circ}\text{C}$ for 2 h. A volume of 20 μ l of protein A agarose was added to each 1 ml of lysate and incubated at 4 $^{\circ}\text{C}$ over 2 nights. The agarose beads bound to the

antibody-protein complex were collected by centrifugation at $14,000 \times g$ at 4°C for 10 min. The supernatants were discarded and the beads washed with PBS and centrifuged at $14000 \times g$ at 4°C three times. Finally the beads were re-suspended in $40 \mu\text{l} \times 2$ sample buffer and electrophoresed using polyacrylamide gels.

Cell counting by trypan blue

In 2D cultures, cells were plated in 24-well tissue-culture plates at a density of 5×10^4 cells in each well. The cells were counted from triplicate wells after days 1, 2, 3, and 4 for MDA-MB-231 and up to day 6 for MCF-7 cells respectively. Cells were then diluted in Trypan Blue (1:1) ratio (vol/vol) and counted using a hemacytometer. For 3D cultures, MCF-7, MDA-MB-231 and MCF10A cells were plated in triplicates in 24-well tissue-culture plates at a density of 25×10^3 cells in each well. The cells were maintained for 8 days before counting. Experiments were repeated at least three times. Statistical significance was determined using one-way ANOVA.

Three-dimensional morphogenesis assay

Cells were plated in 35 mm culture dishes. Ten fields of each well were imaged at $10 \times$ of magnification. Colony morphology was quantified by counting the number of small and spherical colonies versus large ones for MCF-7 and stellate colonies for MDA-MB-231 cells. Spherical colonies versus interconnected tubular like colonies were counted for MCF10A cells. Equal numbers of colonies were counted. Experiments were repeated at least three times. Statistical significance was determined using one-way ANOVA. *P* values less than 0.05 were considered statistically significant.

Invasion assay

Six-well tissue-culture plates were fitted with inserts ($8 \mu\text{m}$ pore size) that have been coated with growth factor-reduced EHS (Matrigel). Endothelial cells (ECV304) were grown in the inserts to confluency, and then seeded with calcein-labeled tumor cells. After 24 h of co-culture, inserts were removed and the endothelial cell layer was gently removed using a cotton swab. The membrane of the insert was then removed and mounted on a microscopic slide and examined by fluorescence microscopy. Fluorescent tumor cells that successfully invaded through the endothelial layer were counted [24].

Immunocytochemistry

For 2D cultures, cells were plated at a density of 1×10^5 cells in each well, on top of glass coverslips. After reaching the desired confluency, slides were blocked for 1 h with 3% (vol/vol) normal goat serum in PBS (NGS, Santa Cruz Biotechnology) and then washed with PBS, and incubated overnight at 4°C with the primary antibody ($1 \mu\text{g/ml}$ in PBS containing 1% NGS). This was followed with PBS washes and a 1 h incubation with an appropriate secondary Alexa-568 conjugated antibody diluted 1:2000. Nuclei were counterstained with Hoechst (DAPI; 4,6-diamino-2-phenylindole) (Molecular Probes, Eugene, OR, USA) and mounted with prolong anti-fade, for analysis using fluorescence microscopy (LSM 410, Zeiss, Germany). For 3D cultures, media was aspirated; cells were fixed with 4% formaldehyde for 20 min at RT, and then permeabilized with 0.5% Triton X-100 in PBS for 10 min at 4°C . Cells were washed with PBS and blocked for 2 h in IF buffer (130 mM NaCl , $7 \text{ mM Na}_2\text{HPO}_4$, $3.5 \text{ mM NaH}_2\text{PO}_4$,

$7.7 \text{ mM Na}_3\text{N}$, 0.1% bovine serum albumin, 0.2% Triton X-100, 0.05% Tween-20) and 10% NGS. Then, cells were incubated with specific primary antibodies ($1 \mu\text{g/ml}$ of blocking buffer) overnight at 4°C . Cells were washed and incubated with secondary Alexa-568 conjugated antibody as above. All immunocytochemistry data were collected from 3 independent experiments. Multiple fields (up to 20) were evaluated per experiment per condition by multiple personnel.

Cell cycle analysis

Cells trypsinized at 70% confluency for 2D cultures and at day 8 for 3D cultures were collected by centrifugation $200 \times g$ for 5 min at 4°C and fixed in ice-cold 70% ethanol for a minimum of 2 h and a maximum of 2 weeks. Cells were then centrifuged ($208 \times g$, 5 min, 4°C) and the pellet was washed with $1 \times$ PBS. DNase free RNase A was added at a concentration of 0.2 mg/ml ($50 \mu\text{l}$) and cells were kept at 37°C in a water bath for 1 h and 30 min to allow full digestion of RNA. The pellet was washed in $1 \times$ PBS before final re-suspension in $420 \mu\text{l}$ of $1 \times$ PBS into flow tubes (BD falcon, USA). $30 \mu\text{l}$ of 2 mg/ml propidium iodide (PI) was then added to each flow tube and the cells were then analyzed using the FACS Vantage SE flow cytometer and cell sorter.

Results

Characterization of Cx43 endogenous expression and localization in human breast tumor cells

The two human mammary adenocarcinoma cells, MCF-7 (moderately invasive) and MDA-MB-231 (highly invasive) were screened for endogenous expression of Cx43. The localization of Cx43 was examined by immunostaining which showed that Cx43 was mainly retained in intracellular compartments (discontinuous white arrows) in both cell lines and rarely deposited on the cell membrane (continuous white arrows) in MCF-7 cells (Fig. 1A). By immunoblotting, Cx43 was detected in cell lysates from MCF-7 and MDA-MB-231 cells as previously reported in the literature with phosphorylated isoforms in MCF-7 (Fig. 1B).

Over-expression of Cx43-EGFP in MCF-7 and MDA-MB-231 cells

In this study, MCF-7 and MDA-MB-231 cells were either transfected with the pEGFP-N1 plasmid containing mouse Cx43 fused to Enhanced Green Fluorescent Protein (EGFP), or with an “empty” pEGFP-N1 plasmid containing only EGFP as a mock control for transfection. The former will be referred to as “Cx43 transfected” cells, and the latter as “sham transfected” cells throughout the remainder of the text. The transfection of both cell lines was verified, at the protein level, by immunoblotting, for expression of Cx43-EGFP or EGFP alone using an anti-Cx43 antibody and a GFP-specific antibody. Probing with the anti-Cx43 antibody revealed a 70 kDa band in Cx43 transfected cells corresponding to the Cx43-EGFP fusion protein, as well as fainter bands around 43 kDa corresponding to endogenous Cx43 in untransfected, sham transfected and Cx43-transfected MCF-7 (Fig. 1B lanes a, b and c) and MDA-MB-231 (Fig. 1B lanes d, e and f) cells. Interestingly, in the case of Cx43-EGFP transfected MDA-MB231 cells, the endogenous levels of Cx43 were down-regulated (Fig. 1B lane f). The EGFP

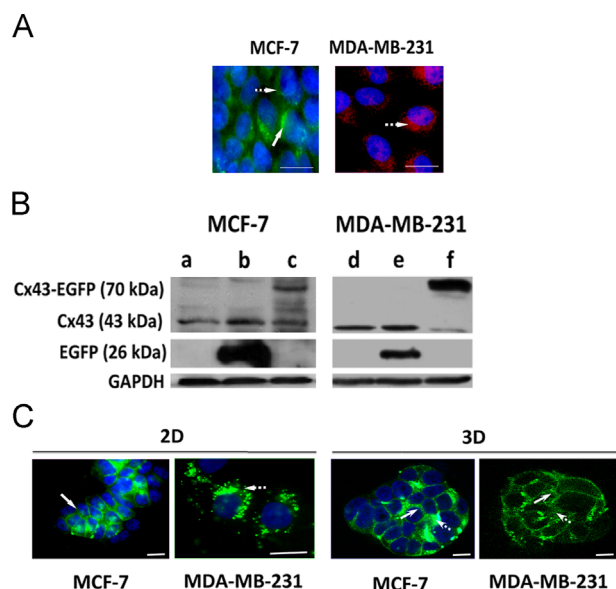


Fig. 1 – Characterization of endogenous Cx43 and transfected Cx43-EGFP expression and localization in human breast tumor cell lines, MCF-7 and MDA-MB-231. (A) Immunofluorescent analysis of MCF-7 and MDA-MB-231 using a Cx43-specific antibody showed prominent diffused cytosolic localization in both cell lines (white discontinuous arrows) and rare membranous (white arrows) localization in MCF-7 cells. The micrographs reveal nuclei stained with Hoechst 33342 merged with Cx43 staining. Scale bar corresponds to 20 μm . (B) Western blots of total cellular extracts of MCF-7 and MDA-MB-231 cells respectively; untransfected (a and d), sham-transfected (b and e) and Cx43-EGFP transfected (c and f) using anti-Cx43 and anti-GFP antibodies. The molecular weights of respective proteins are indicated. The anti-GFP antibody showed EGFP (26 kDa) in sham transfected cells (b and e) and exogenous Cx43-EGFP (70 kDa) in Cx43 transfectants (data not shown). GAPDH demonstrates equal protein loading. The anti-Cx43 antibody detected the 70 kDa Cx43-EGFP as well in Cx43 transfected cells (c and f) as well as the 43 kDa band corresponding to endogenous Cx43 in sham transfected and untransfected cells. (C) Localization of Cx43-EGFP in 2D and 3D cultures of MCF-7 and MDA-MB-231 cells. Cx43-EGFP shows membranous (continuous arrows) and vesicular localization (discontinuous arrows) in 2D cultures of MCF-7 and 3D cultures of both MCF-7 and MDA-MB-231 cells compared to predominantly vesicular localization in 2D cultures of MDA-MB-231 cells. Scale bar corresponds to 20 μm .

antibody detected both 70 kDa band and EGFP at 26 kDa in Cx43 transfected cells (Fig. 1B lanes c and f) while only a 26 kDa (Fig. 1B lanes b and e) in the sham transfected cells. To enrich the Cx43-EGFP expressing cells and generate a population with expression levels comparable to sham transfected cells, FACS was performed for two consecutive rounds for both cell lines. Fluorescent microscopy showed that Cx43-EGFP localized at both the membrane (continuous white arrow heads) and intracellular vesicles (discontinuous white arrow heads) in both 2D and 3D cultures of MCF-7 cells (Fig. 1C). In MDA-MB-231 cells however, Cx43-EGFP showed punctate fluorescence restricted to intracellular vesicles when

grown in 2D cultures as previously reported in the literature [5]. In contrast, Cx43-EGFP exhibited prominent membranous deposition when cells were cultured in Matrigel (Fig. 1C).

Cx43-EGFP over-expression decreases proliferation of human breast tumor cells by modifying their cell cycle progression

Since Cx43 is generally expected to reduce tumor growth, we assessed the effect of Cx43-EGFP over-expression on MCF-7 and MDA-MB-231 cellular growth and proliferation on plastic (2D) and in Matrigel (3D). Cell counts were monitored using the trypan blue dye exclusion assay over a period of 6 days for MCF-7 and 4 days for MDA-MB-231 cell grown in 2D cultures and for 8 days in 3D cultures of both cell lines. Cx43-EGFP decreased MCF-7 cellular growth up to 50% by day 6 in 2D cultures and up to 80% by day 8 in 3D cultures (Fig. 2A). In contrast, whereas MDA-MB-231 cells grown in 2D cultures did not show difference in growth rate between untransfected, sham-transfected and Cx43-EGFP transfected cells, Cx43-EGFP overexpression significantly decreased the growth rate of MDA-MB-231 cells by 30% when cultured in Matrigel (Fig. 2A). The number of dead cells did not exceed 2% and did not differ between transfected and untransfected cells in both cell lines.

In addition, photomicrographs taken at day 8 after plating cells in Matrigel revealed a difference in morphology of Cx43-EGFP transfected MCF-7 cells as compared to sham transfected and untransfected cells (Fig. 2B). In fact, cluster size grouping, based on cluster diameter, showed that small sized clusters (diameter between 10–35 μm) were abundant in Cx43-EGFP transfected cells versus sham transfected and untransfected MCF-7 cells. Moreover, large sized clusters (diameter larger than 75 μm) were not as abundant in Cx43-EGFP transfected MCF-7 cells when compared to untransfected and sham eGFP transfected cells (Fig. 2C).

As for MDA-MB-231 cells, the majority of untransfected and sham-transfected cells formed stellate colonies in Matrigel, whereas cells over-expressing Cx43-EGFP grew into spherical colonies that resemble the growth morphology of normal mammary epithelial cells in Matrigel (Fig. 2B). By counting stellate and spherical colonies that formed at days 3, 5 and 8 in 3D cultures of untransfected, sham-transfected and Cx43-EGFP MDA-MB-231 transfected cells, cells overexpressing Cx43-EGFP formed 30–40% less stellate colonies than sham-transfected and untransfected cells (Fig. 2C).

In order to establish whether Cx43-EGFP over-expression affects cell cycle progression of both tumor cell lines given that it affected their proliferation rate, PI cell cycle analysis was performed on untransfected, sham transfected and Cx43-EGFP transfected MCF-7 and MDA-MB-231 cells at 70% confluence. Cx43-EGFP overexpression induced a 25% increase of S-phase of MCF-7 Cx43-EGFP transfected cells in both 2D and 3D cultures (Fig. 2D) and a decrease of about 4% in S1 cells and 14% in G2/M cells. In addition, cell doubling time of MCF-7 in 2D cultures increased from 24 h to 36 h (not shown). As mentioned previously, MDA-MB-231 cells in 2D cultures did not show difference in growth rate or morphology between untransfected, sham-transfected and Cx43-transfected cells. In accordance with that, Cx43-EGFP overexpression in MDA-MB-231 cells exhibited no significant effect on the percentage of cells progressing throughout any cell cycle phase as compared to sham-transfected and

untransfected MDA-MB-231 cells when grown in 2D cultures. However, when cultured in Matrigel Cx43-EGFP over-expression in MDA-MB-231 cells induced a 28% increase of G0/G1 cell-cycle phase when compared to sham-transfected and untransfected MDA-MB-231 cells (Fig. 2D).

Cx43-EGFP over-expression reduces the transendothelial invasive potential of human breast tumor cell lines

Since Cx43-EGFP overexpression affected cellular growth and morphology of MCF-7 and MDA-MB-231 cluster growth, we set to determine whether Cx43-EGFP also affected the transendothelial invasive ability of these cells. Accordingly, extravasation was performed by seeding equal numbers of untransfected and transfected MDA-MB-231 cells labeled with calcein dye over a uniform layer of endothelial cells, as explained in Materials and Methods. Twenty four hours after co-culturing the cells, it was evident that Cx43-transfected MCF-7 and MDA-MB-231 cells were less able to extravasate across the endothelial cell layer (Fig. 3A) and to invade through the Matrigel basement membrane components. Cell counting of MCF-7 cells, labeled with calcein dye, showed that Cx43-EGFP transfected cells exhibited reduced invasive ability by 58%, when compared to untransfected and sham transfected MCF-7 cells. In addition, cell counting of calcein dye labeled invaded MDA-MB-231 cells showed that Cx43-EGFP transfection reduced cell invasiveness by ~30%, when compared to sham transfected, and untransfected cells (Fig. 3B).

Truncated Cx43-EGFP does not decrease proliferation and transendothelial migration in human breast tumor cells

To assess the contribution of Cx43 cytosolic domain, binding site of Cx-associated proteins, in mediating its tumor suppressive effects, MCF-7 and MDA-MB-231 cells were transfected with a

C-terminus truncated version of Cx43 at amino acid 242 fused to EGFP. As noted above in Fig. 1C for Cx43-EGFP membrane localization in MCF-7 cells, the truncated Cx43-EGFP in these –7 cells also localized to the membrane (Fig. 4A). In contrast to Cx43-EGFP transfected MCF-7 cells which showed slower proliferation and impeded invasion, those transfected with the truncated Cx43-EGFP showed similar proliferation and invasion potential as that of sham transfected MCF-7 cells (Fig. 4A). MDA-MB-231 cells expressing the truncated Cx43-EGFP showed similar distribution as those expressing the Cx43-EGFP which was restricted to the cytosol and intracellular vesicles (Figs. 1C and 4A). Cell counts on day 4 of culture did not show differences among sham, Cx43 and truncated-Cx43 transfected cells (Fig. 4A).

Overexpressing both Cx43-EGFP and truncated Cx43-EGFP in MCF-7 cells induced an increase in the GJIC, by Lucifer yellow dye transfer assay, compared to sham transfected MCF-7 cells. Treating full length Cx43-GFP transfected cells with 18 α -glycerrethnic acid (inhibitor of GJIC) did not revert their decreased growth rate compared to untreated control cells (data not shown), thereby suggesting a GJ independent tumor suppressive role of Cx43.

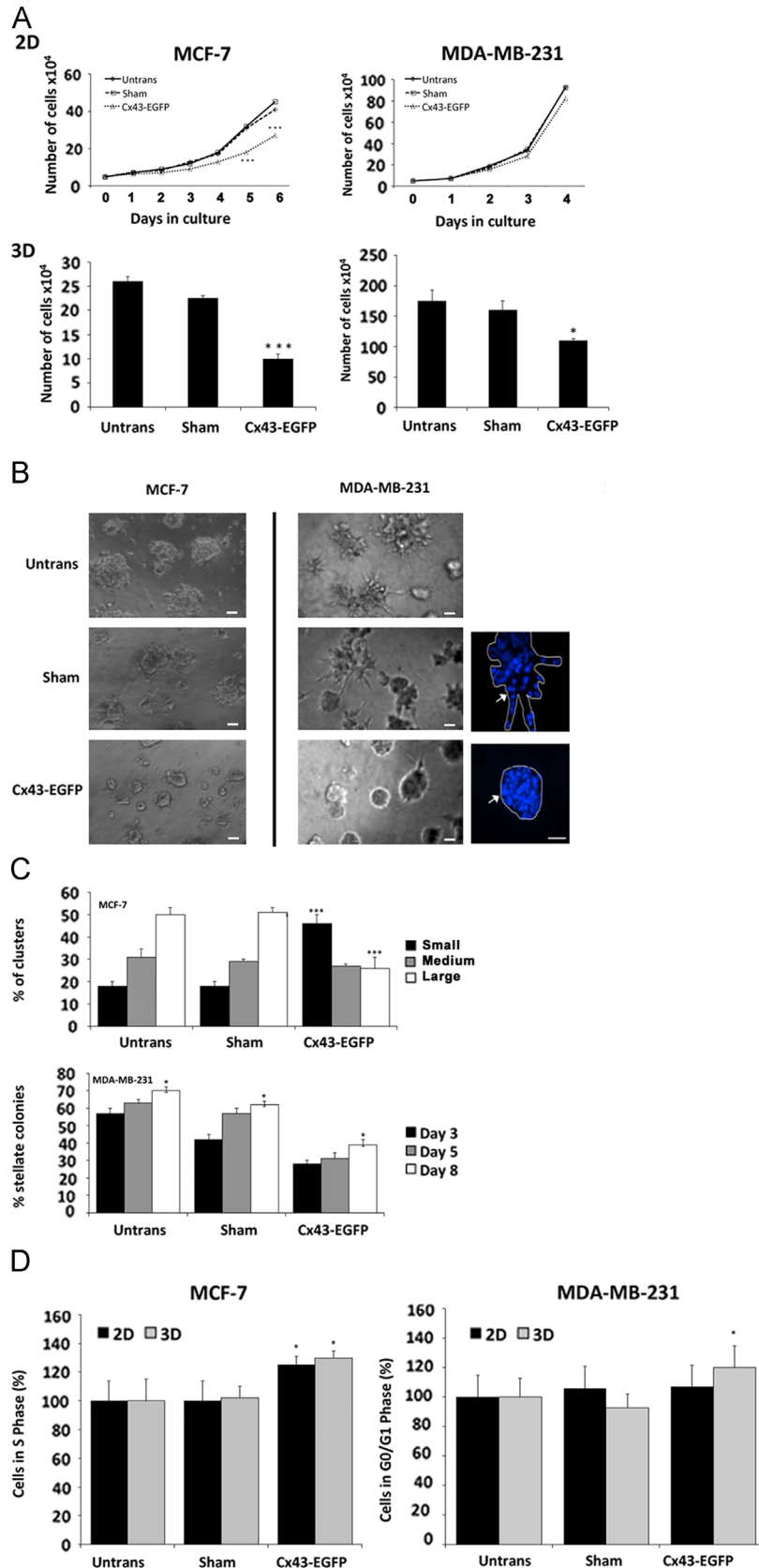
ShRNA-Cx43 induces a tumor-like phenotype in MCF10A cells, nonneoplastic human breast epithelial cells

In order to further illustrate the tumor suppressive role of Cx43 in the mammary epithelium, Cx43 was stably silenced in MCF10A cells as revealed by Western blot and qRT-PCR (Fig. 4B). The effect of Cx43 silencing on both 2D and 3D proliferation and morphology of MCF10A cells was assessed. In 2D cultures, shRNA-Cx43 transfected MCF10A cells showed a 53% increase by day 5 compared to untransfected and shRNA-scr transfected ones. In 3D culture, shRNA-Cx43 transfected cells showed a 38% increase in proliferation at day 8 of culture compared to untransfected and shRNA-scr transfected cells (Fig. 4B).

Fig. 2 – Effect of Cx43-EGFP over-expression on the proliferation and cell cycle progression of human breast tumor cell lines, MCF-7 and MDA-MB-231 in 2D and 3D culture conditions. (A) Graphs representing the total number of MCF-7 and MDA-MB-231 cells. In 2D cultures, MCF-7 cells transfected with Cx43-EGFP showed a 56% decrease in total cell number compared to untransfected and sham-transfected counterparts by day 6, whereas Cx43-EGFP transfected MDA-MB-231 cells did not show any difference in total cell number by day 4 of culture. Cell counts in 2D cultures were determined on daily basis until untransfected, sham-transfected cultures of MCF-7 and MDA-MB-231 cells reached confluency. On day 8 of culture in 3D cultures, MCF-7 cells transfected with Cx43-EGFP showed an 80% decrease in total cell number compared to sham-transfected counterparts, whereas Cx43-EGFP transfected MDA-MB-231 cells exhibited a 35% decrease in total cell number when compared to sham-transfected and untransfected counterparts. Statistical analysis obtained from three independent experiments revealed statistical significance at $p < 0.05$ represented by one asterisk and at $p < 0.001$ by three asterisks. (B) Photomicrographs of 3D cultures of MCF-7 cells revealed a decrease in cluster size in Cx43-EGFP transfected cells when compared to sham and untransfected cells. Cx43-EGFP transfected MDA-MB-231 cells grew into spherical colonies as compared to stellate colonies of their sham and untransfected counterparts. Representative micrographs of Hoechst stained MDA-MB-231 clusters indicates the difference in 3D growth of stellate structured colonies of sham transfected MDA-MB-231 cells versus spheroid clusters of Cx43-EGFP overexpressing MDA-MB-231 cells. Scale bars for MCF-7 and MDA-MB-231 correspond to 100 μ m. (C) Histogram showing the percent of small (< 35 μ m length of diameter, medium (between 35 and 75 μ m) and large (> 75 μ m) colonies of untransfected, sham and Cx43-EGFP transfected MCF-7 at day 8 of culture. The MDA-MB231 cells' histogram shows the percent stellate colonies of untransfected, sham, and Cx43 transfected MDA-MB-231 cells at days 3, 5 and 8 of culture. Statistical analysis obtained from three independent experiments revealed statistical significance at $p < 0.05$ represented by one asterisk and at $p < 0.001$ by three asterisks. (D) Histograms showing percentage of MCF-7 and MDA-MB-231 cells in S and G0/G1 phases of the cell cycle respectively). Exogenous Cx43 prolongs S-phase of the cell cycle by 25% in both 2D and 3D cultures of MCF-7 cells. No effect of Cx43 exogenous expression on cell cycle progression of MDA-MB-231 cells in 2D cultures but it prolonged G0/G1 phase under 3D culture conditions. Percentages of cells were normalized to untransfected cells. Statistical analysis obtained from three independent experiments revealed statistical significance at $p < 0.05$ represented by an asterisk.

Moreover, untransfected and shRNA-scr transfected MCF-10A cells formed in 3D cultures spherical clusters (white arrow), and shRNA-Cx43 transfected cells formed interconnected tubular-like colonies

(black arrow) at day 8 of culture (Fig. 4B). Indeed, counting tubular-like and spherical colonies showed that shRNA-Cx43 transfected cells formed ~50% less spherical clusters than control cells as they



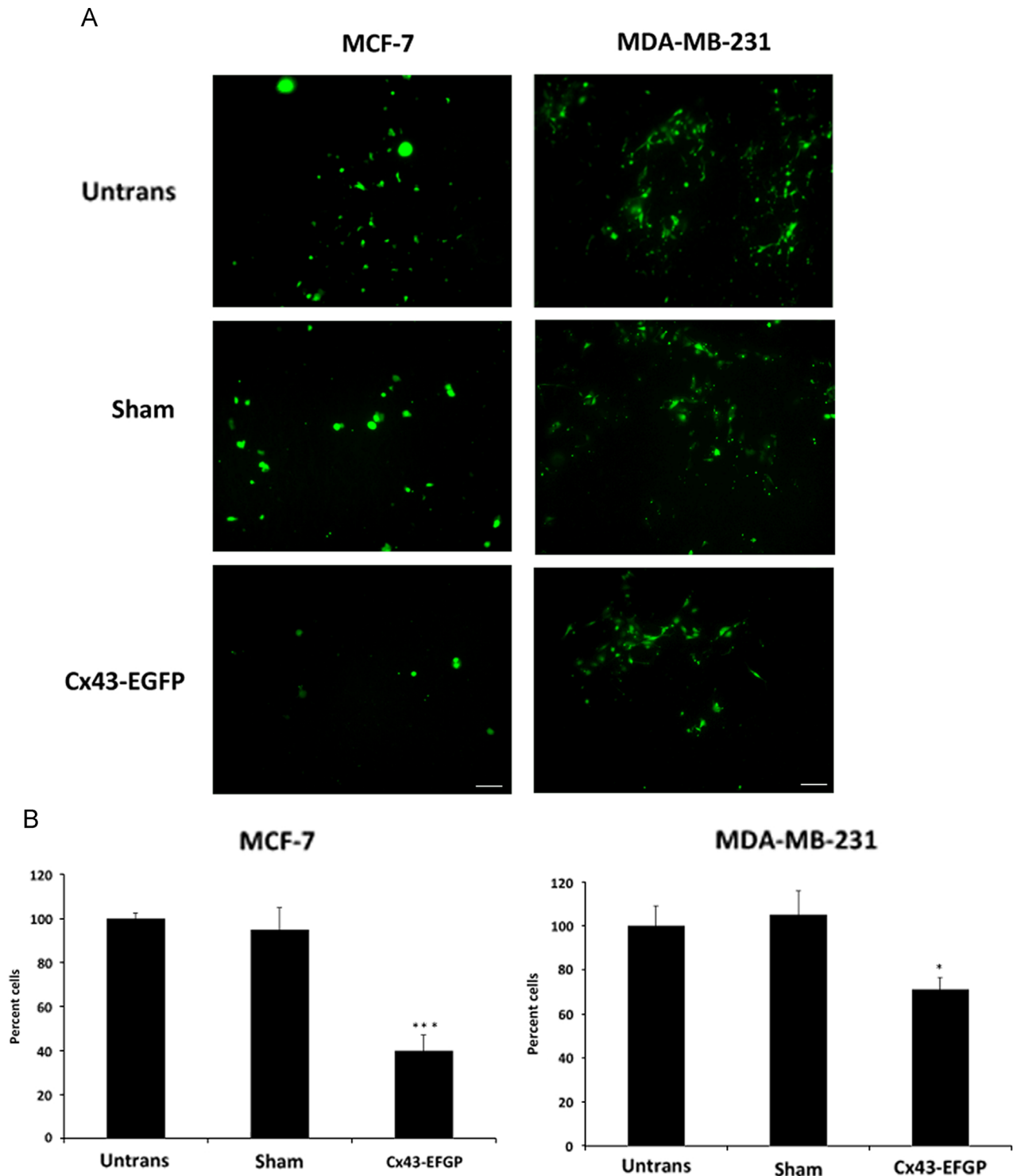


Fig. 3 – Effect of Cx43-EGFP over-expression on the transendothelial invasive potential of human breast tumor cell lines. (A) Fluorescent photomicrographs of calcein labeled MCF-7 and MDA-MB-231 cells that invaded through endothelial cells and matrix components. (B) Histograms showing percentage of invaded cells for untransfected, sham and Cx43-EGFP transfected MCF-7 and MDA-MB-231 cells. Statistical analysis obtained from three experiments that revealed significant differences at $p < 0.05$ are represented by asterisk (*) and at $p < 0.001$ by (***) . Scale bar corresponds to 100 μm .

formed tubular-like colonies instead. Interestingly, these changes in growth morphology were also associated with loss of lumen formation in shRNA-Cx43 transfected cells. In fact, whereas spherical clusters in control cells had a lumen, typical of MCF10A, shRNA-Cx43 transfected spherical clusters showed no lumen (Fig. 4B).

Cx43-EGFP overexpression restores membranous localization and association of β -catenin, α -catenin and ZO-2

Previous studies from our lab have shown that under conditions favoring mammary epithelial differentiation, β -catenin was

sequestered by GJ complexes at the membrane and away from the nucleus. Moreover, we also showed that α -catenin and ZO-2, which are also Cx-associated proteins known to have dual roles in signaling and adhesion, assembled at the membrane with Cx43 under differentiation permissive conditions [19]. To explore the effect of Cx43-EGFP overexpression on GJ complex assembly immunoblotting, immunolabeling and co-immunoprecipitation analyses were performed. Collectively, data from these assays are adequate indicators for the assembly of the GJ complex at the membrane. Western blots of total cellular extracts probed with antibodies for β -catenin, α -catenin and ZO-2 showed that the levels of these proteins were not altered among transfected, sham transfected and untransfected MCF-7 and MDA-MB-231 cells cultured under 2D and 3D conditions (Fig. 5A). Moreover, indirect immunocytochemistry in 2D and 3D cultures for β -catenin demonstrated membranous localization across different transfectants of MCF-7 (Fig. 5B). Co-localization studies showed that β -catenin co-localized with Cx43-EGFP in 2D and 3D cultures of MCF-7 cells (Fig. 5C). As for MDA-MB-231 cells, the localization of β -catenin was not altered by Cx43-EGFP over-expression in 2D cultures and was mostly intracellular with some weak membranous deposition. In fact nuclear as well cytosolic staining of β -catenin was noted in 2D cultures of sham and Cx43-EGFP transfected MDA-MB231 cells. In contrast, β -catenin localization was clearly membranous in 3D spherical clusters of Cx43-transfected MDA-MB-231 cells, unlike the case of sham transfected and untransfected stellate clusters (Fig. 5B).

To determine the effect of Cx43-EGFP overexpression on the complex assembly at the membrane in both cell lines, co-immunoprecipitation studies were performed to determine whether Cx43-EGFP associates with β -catenin, α -catenin and ZO-2 in 2D and 3D cultures transfected MCF-7 and MDA-MB-231 cells. Interestingly, whereas Cx43-EGFP associates with β -catenin, α -catenin, and ZO-2 in 2D and 3D cultures of Cx43-EGFP transfected MCF-7 cells, no association occurred between Cx43-EGFP and β -catenin, α -catenin or ZO-2 in 2D cultures of MDA-MB-231 cells. On the other hand Cx43-EGFP associated with β -catenin, α -catenin and ZO-2 in 3D culture conditions of MDA-MB-231 cells only (Fig. 6A).

Given that the fundamental processes required for mammary gland differentiation are usually deregulated in breast cancers we sought to determine whether the tumor-suppressive role played by Cx43 is paralleled by a decrease in nuclear levels of β -catenin due to its sequestration at the membrane and away from the nucleus, hence limiting its transcriptional-mediated effects in the nucleus. Indeed, analysis of nuclear extracts of both tumor cell lines showed that β -catenin nuclear levels are significantly reduced only under conditions when Cx43-EGFP is membranous and associating with β -catenin; namely in 2D and 3D cultures of Cx43-EGFP expressing MCF-7 cells as well as in 3D cultures of Cx43-EGFP transfected MDA-MB-231 cells (Fig. 6B).

Discussion

Intercellular adhesion is essential for the maintenance of cellular organization and proper tissue physiology. Junctional molecules do not only provide structural integrity, but also act as signaling hubs integrating signals from external stimuli, or even from within the cell [25,26]. Amongst cellular adhesion complexes, GJs have the unique ability to mediate intercellular transfer of

molecules between cells, a phenomenon coordinating a plethora of cellular responses ranging from cell survival to normal tissue homeostasis and synchronization [27]. Nevertheless, Cxs also exhibit various channel-independent functions that control other processes such as cellular growth, apoptosis and differentiation [28,11].

Cell-cell adhesion molecules are highly regulated during development and differentiation [16], and their disruption is associated with various diseases. In cancer, junctional molecules are usually found mutated, down-regulated, or mis-localized [29]. Interestingly, GJ assembly and Cx expression are differentially regulated throughout the different stages of tumor progression [22,30]. Whereas Cx26 and Cx43 are usually down-regulated in primary mammary tumors [4,31–34], these same Cxs are up-regulated during later stages of breast carcinogenesis [35]. This suggests that during early tumorigenic stages, GJ down-regulation may contribute to tumor cell detachment, proliferation and intravasation, and that GJ expression and assembly during later metastatic stages may facilitate extravasation and secondary tumor formation [30,36].

Several studies have shown that Cx over-expression in cell lines of primary mammary tumor origin decreases their growth rates and inhibits their invasive abilities [5–9,23,37], and that Cx down-regulation increases cellular malignancy [10], hence establishing a tumor suppressive role for Cxs in primary tumors. Nevertheless, the mechanism governing this effect is not completely understood, and has been reported to be GJIC-dependent [9] as well as GJIC-independent by different groups [5,8,23]. In this study, we aim to unravel the mechanism mediating the tumor suppressive effect of Cx43, the major Cx expressed in the mammary gland, in 2D and 3D cultures of two breast adenocarcinoma cell lines: MDA-MB-231 (highly invasive) and MCF-7 (moderately invasive). We had previously shown that mammary epithelial cell differentiation involves the assembly of GJ complexes comprising α -catenin, β -catenin, and ZO-2 at the cellular membrane, with β -catenin being sequestered away from the nucleus where it promotes cellular proliferation [19,26]. Given that the fundamental processes required for mammary gland development and differentiation are usually deregulated in breast cancers [21], we set to determine whether Cx43 overexpression would attenuate breast adenocarcinoma growth and invasiveness by sequestering β -catenin at the membrane and limiting its downstream tumor promoting effects.

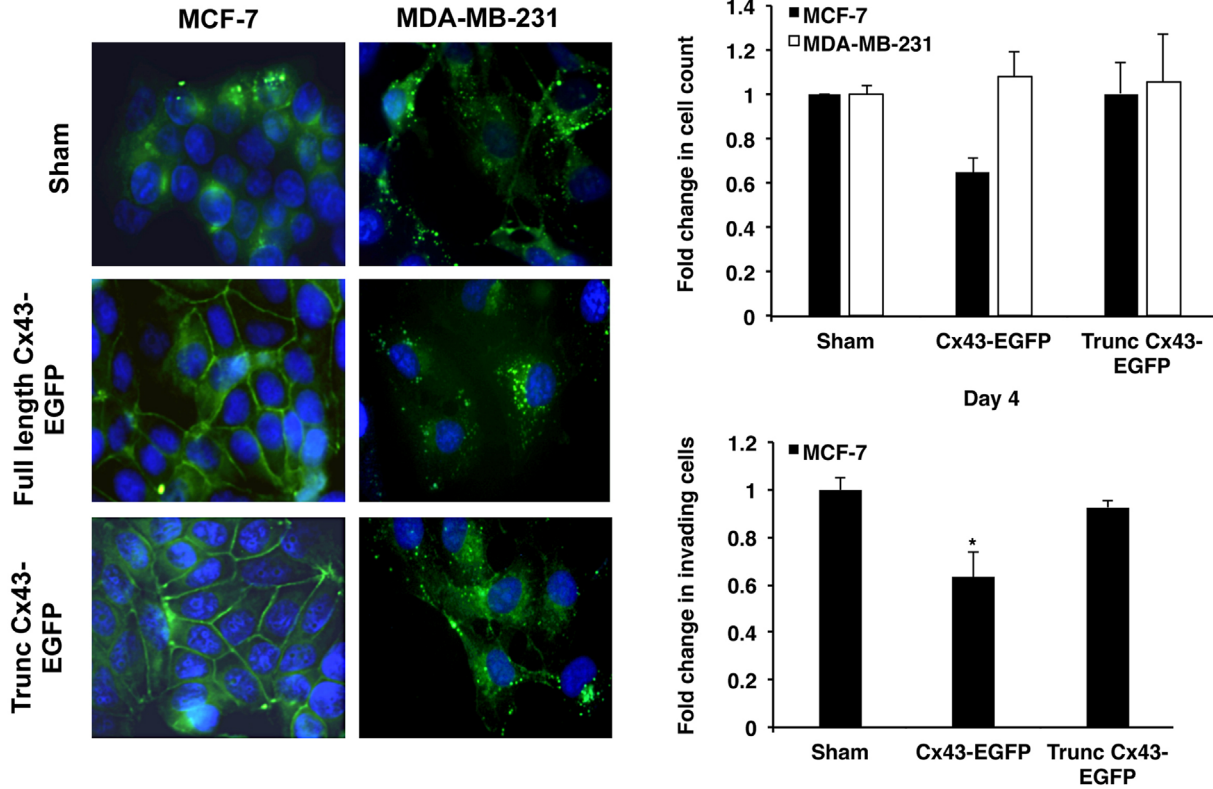
As an initial step, we characterized the levels and localization of endogenous Cx43 in MDA-MB-231 and MCF-7 cells. We chose to utilize both cell lines since they have different degrees of invasiveness and because of their widespread usage as breast cancer research models. Western blot analysis showed that both cell lines express Cx43, and indirect immunocytochemistry revealed predominant intra-cellular localization of Cx43 in both cell lines, with some rare membranous deposition in MCF-7 cells. This finding is in line with studies reporting that cells derived from primary tumors usually show cytosolic Cx localization or down-regulation of Cx expression altogether [3,38]. Moreover, it confirms that both of these cell lines represent good models to study the effect of exogenous Cx43 over-expression and its assembly into GJ complexes on tumorigenic properties, as endogenous Cx43 expressed by these cells does not prominently assemble into membranous GJs [5,23]. Whether the level of phosphorylation in MCF-7 cells modulates the limited membrane deposition and GJ functionality was not assessed.

Previously, we reported that in CID-9 cells and in SCp2 mammary cells Cx43 phosphorylation correlated with GJ functionality and association with catenins and ZO-2 protein [17,19] and its phosphorylation levels were modulated in the rodent mammary gland during

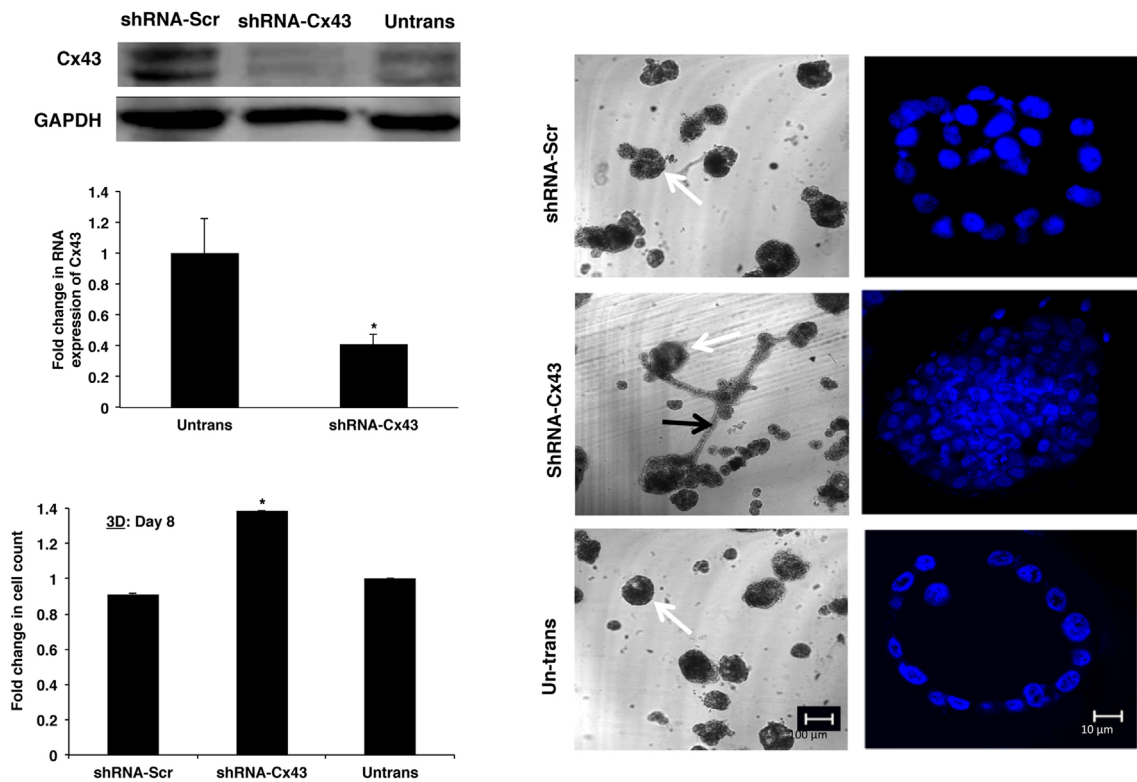
lactation [16]. As such, we proceeded to over-express Cx43-EGFP in both cell lines.

Since tumor suppressive effects of Cx re-introduction into cancer cells, particularly in the MDA-MB-231 cell line, have been

A



B



shown in 3D cultures as well as *in vivo* [23], we sought to assess the effect of Cx43-EGFP over-expression on the growth and proliferation of both cell lines cultured under 2D and 3D culture conditions. In line with previous reports [23], our results showed that while Cx43-EGFP over-expression decreased the growth of 2D and 3D cultures of MCF-7 cells, MDA-MB-231 proliferation was impeded only under 3D culture conditions. A reduction in proliferation rate in both 2D and 3D conditions was also demonstrated in HT29 cells, colon cancer cells, upon the ectopic expression of Cx43 [39]. Importantly, no difference in cell death was noted among transfected and untransfected cells, hence establishing that Cx43-EGFP overexpression did not induce apoptosis *via* its interaction with Bak, Bcl-xL and Bax [40,41], or via GJIC-mediated propagation of death signals as previously reported [42,43]. Interestingly, truncated Cx43, although capable of membrane localization did not decrease proliferation of MCF-7 cells suggesting that the anti-proliferative effect of Cx43 requires an intact C-terminus. Proliferation was not noted in MDA-MB-231 cell line transfected with truncated Cx43-EGFP, Cx43-EGFP and sham, confirming previous studies which showed that differences in proliferation of MDA-MB-231 cells following exogenous connexin expression were only observed in 3D culture systems [23].

Studies in our laboratory have demonstrated that Cx43-silenced MCF10A nonneoplastic human breast cells showed an increased proliferation rate in both 2D and 3D cultures compared to control cells. This is in accordance to a similar finding in a recent study by Gangozo et al. [44] where they demonstrated that the down-regulation of Cx43 in cultured astrocytes promoted higher proliferation rate. Given all the above, the tumor suppressive effect of Cx43 requires its localization to the membrane and a C-terminus to interact with Cx associated proteins. The effect is displayed in a cell-specific and context-dependent manner.

Moreover, Cx43-EGFP over-expression induced differences in growth morphology of MDA-MB-231 and MCF-7 cells when cultured in Matrigel. Whereas the majority of untransfected MCF-7 cells formed large spherical colonies and MDA-MB-231 cells formed stellate colonies as previously described for the MDA-MB-231 cell line [23], MCF-7 cells over-expressing Cx43-EGFP formed smaller sized spherical clusters and Cx43-EGFP expressing MDA-MB-231 cells grew in compact spherical clusters that more resembles the acinar growth of normal mammary

epithelial cells. Interestingly, spherical colonies formed by both cell lines did not form lumens (not shown) hence indicating that the over-expression of Cx43-EGFP induced only partial reversion of their malignant phenotype [23]. Cx43-silenced MCF10A cells showed a disrupted lumen structure in contrast to control MCF10A cells that displayed a typical lumen structure enclosed within a single layer of mammary epithelial cells. In addition, Cx43 silencing induced a change in 3D growth morphology of MCF10A colonies where there is an evident shift from the spheroid colonies to tubular connected growth morphology.

Knowing that cell junctions mediate proper morphogenesis of mammary epithelium as illustrated by loss of normal acinar architecture and initiation of tumorigenesis upon tight junctions destabilization [45]; our findings support a critical role for Cx43, a main cell junction protein, in sustaining a normally differentiated breast epithelium.

Given that cell cycle progression has been shown to be affected by Cx expression [11], we set to determine whether changes induced by Cx43-EGFP over-expression in MCF-7 and MDA-MB-231 can be correlated with changes in cell cycle progression. Whereas Cx43-EGFP transfected MCF-7 cells showed an increased cell population in the S-phase and reduced population of cells in G0/G1 and G2/M phases under both 2D and 3D cultures, Cx43-EGFP over-expression in MDA-MB-231 cells increased cell population in G0/G1 cell-cycle phase only when cultured under 3D conditions. This finding suggests that Cx43 over-expression may affect different cell cycle phases in different cell lines. For instance, whereas Cx43 overexpression has been shown to prolong G1 phase in U2OS cells by increasing p27 levels [7], and to prolong S-phase in rat insulinoma cells [46], it was shown to prolong the G1 and S phases in HEK293T cells when paralleled by N-cadherin overexpression [47]. Worth noting is that although transfected MDA-MB231 cells in 3D cultures showed consistent increase of cells in G0/G1 phases, the effect on other phase varied. This requires further investigation. Nevertheless, given that our experiments were performed on non-synchronized cells, synchronizing our transfectants would allow a more accurate quantification of the amount of cells trapped in the different cell cycle phases [48,49].

Cx43 transfected MCF-7 and MDA-MB-231 cells were both less able to extravasate through endothelial cells and basement membrane

Fig. 4 – Effect of truncated Cx43 overexpression on proliferation of human breast tumor cells and silencing of Cx43 on morphology and proliferation of nonneoplastic human breast cells. (A) Truncated Cx43-EGFP does not mediate anti-proliferative effects in human breast tumor cells. Expression and localization of the different constructs in MCF-7 and MDA-MB-231 cells. Cx43-EGFP and truncated Cx43-EGFP transfected MCF-7 cells show mainly membranous (arrow heads) and limited cytosolic localization of the plasmid-encoded protein, while GFP is diffused in the cytosol in sham transfected MCF-7 cells. In contrast to truncated (Trun) Cx43-EGFP expression the expression of Cx43-EGFP decreased MCF-7 proliferation at day 4 of culture as revealed by the fold change in cell count (top graph). It also resulted in a decreased invasion as compared to sham and truncated Cx43-EGFP transfected MCF-7 (bottom graph). MDA-MB-231 cells transfected with Cx43-EGFP, and truncated Cx43-EGFP showed a similar pattern of cytosolic localization of the plasmid-encoded protein. Cx43-EGFP expression did not induce a decrease in cell proliferation in MDA-MB-231 after 4 days in culture (top graph). (B) Cx43 silencing induces a decrease in proliferation rate and a change in 3D morphology of MCF10A colonies. Western blot and qRT-PCR (top graph) shows a decrease in the expression levels of Cx43 at the protein and RNA levels, respectively, in cells with shRNA-Cx43 compared to control cells. The bottom bar graph shows the fold change in cell number of shRNA-Cx43 transfected cells. The phase contrast photomicrographs on the right indicate the change in growth morphology from spherical colonies (white arrow) in untransfected and shRNA-Scr transfected cells to tubular-like colonies (black arrow) in shRNA-Cx43 transfected cells on day 8 of culture. DNA specific dye (Hoechst 33342) staining in z-sections shows that spherical clusters transfected with shRNA-Cx43 have no lumen compared to the untransfected and shRNA-Scr control groups. Statistical analysis obtained from three experiments that revealed significant differences at $p < 0.05$ are represented by asterisk (*) and at $p < 0.001$ by ().**

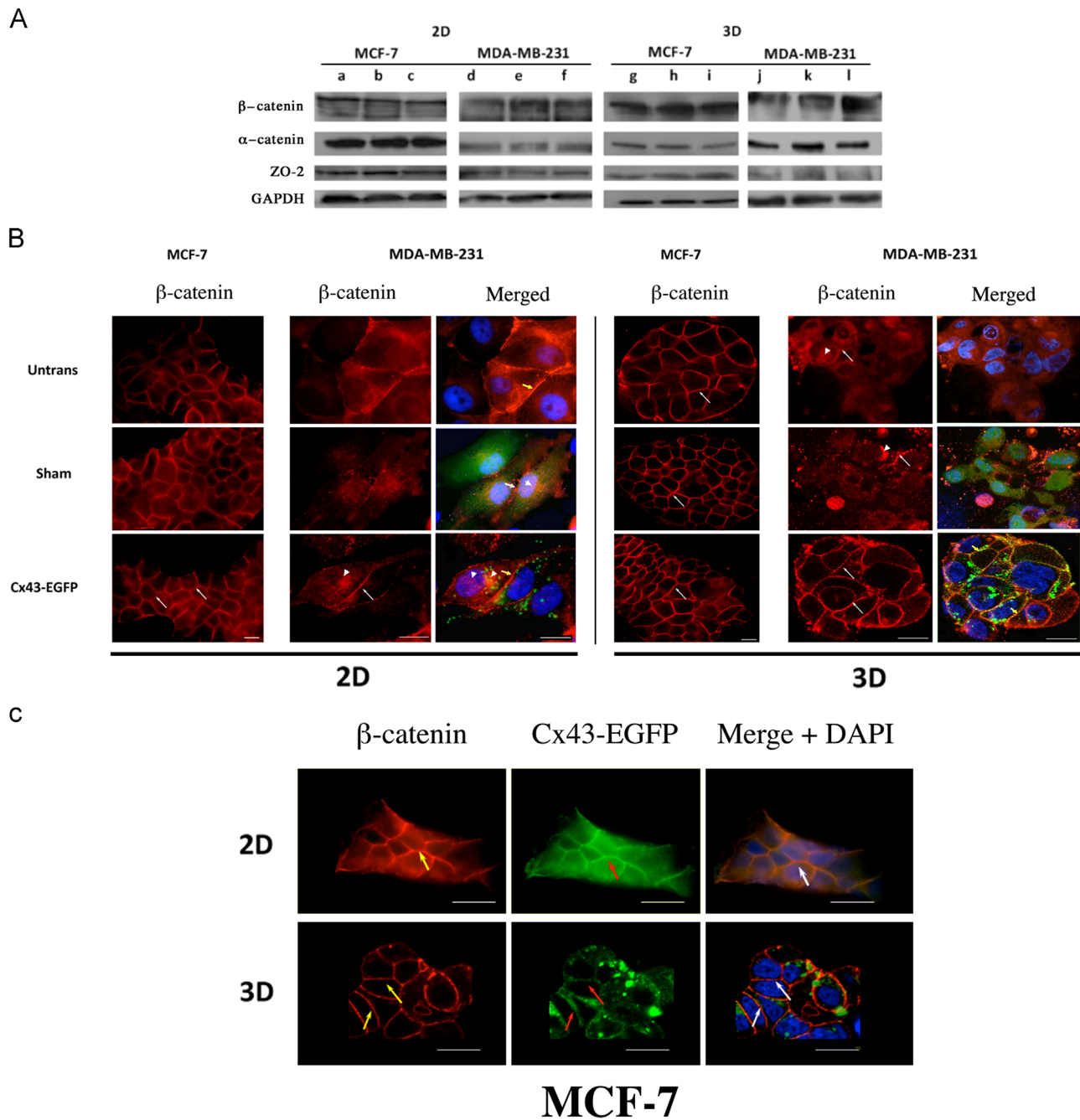


Fig. 5 – Effect of Cx43-EGFP overexpression on the total levels and localization of β -catenin in 2D versus 3D cultures of MDA-MB-231 and MCF-7 cells. (A) Western blots showing expression of β -catenin, α -catenin and ZO-2 in 2D and 3D cultures of untransfected (a and g), sham (b and h) and Cx43-EGFP transfected (c and i) MCF-7 cells and untransfected (d and j), sham (e and k) and Cx43-EGFP transfected (f and l) transfected MDA-MB-231 cells respectively. GAPDH demonstrates equal protein loading. Western blots of total extracts show that the levels of β -catenin, α -catenin and ZO-2 are not affected by Cx43 over-expression in MCF-7 and MDA-MB-231 cells under 2D and 3D conditions. (B) Immunofluorescence of MCF-7 and MDA-MB-231 cells stained using a β -catenin specific antibody shows membranous localization in both 2D and 3D cultures of untransfected, sham and Cx43-EGFP transfected MCF-7 cells. As for MDA-MB-231 cells, co-localization images revealed cytosolic and nuclear β -catenin localization (arrow head) as well as limited membranous deposition (arrows) in 2D and 3D cultures of untransfected and sham transfected cells and membranous localization in Cx43-EGFP transfected cells (arrows). (C) Co-localization images for β -catenin and Cx43-EGFP in 2D and 3D transfected cells show overlapping membranous distribution (arrows). Scale bars correspond to 20 μ m.

components. Although some studies report that Cx over-expression in malignant cells enhanced their invasive abilities [50,7], other studies showed that reintroduction of Cxs into Cx-deficient cell lines

downregulated their invasive abilities [51,52], and are thus in line with our finding. Our results also indicate that Cx43 silencing in MCF10A cells altered their morphology and increased their migratory

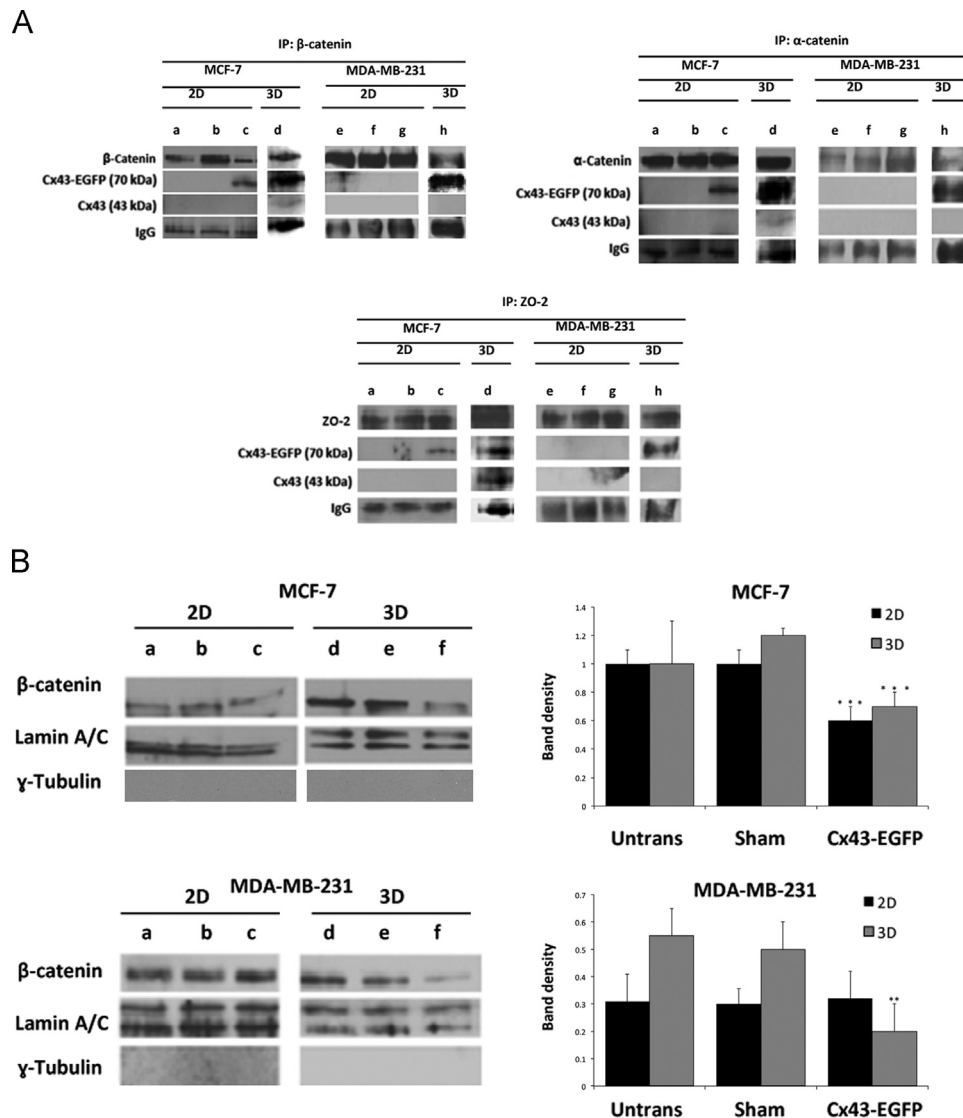


Fig. 6 – Cx43-EGFP assembles into GJ complexes that sequester β -catenin away from the nucleus. (A) Immunoprecipitation using anti β -catenin, anti- α -catenin or anti-ZO-2 antibody followed by Western blots for Cx43 in MCF-7 and MDA-MB-231 cells grown in 2D and 3D conditions. There was no association between Cx43 and β -catenin, α -catenin and ZO-2 in 2D cultures of untransfected and sham MCF-7 (a and b) and 2D cultures of untransfected, sham and Cx43-EGFP transfected MDA-MB-231 (e, f and g) cells. On the other hand, Cx43-EGFP associated with β -catenin, α -catenin and ZO-2 in 2D cultures of Cx43-EGFP transfected MCF-7 (c) and 3D cultures of both Cx43-EGFP transfected MCF-7 (d) and MDA-MB-231 (h) cells. IgG was used for antibody-protein specific precipitation. (B) Western blots of nuclear cell extracts show that the nuclear levels of β -catenin are decreased by Cx43-EGFP over-expression in 2D and 3D cultures of MCF-7 cells (c and f) as compared to untransfected (a and d) and sham (b and e) transfected cells. (C) There was no change in β -catenin levels in 2D and 3D cultures of untransfected (a and d), sham transfected (b and e) MCF-7 and in 2D cultures of Cx43-EGFP (c) transfected MDA-MB-231 cells as compared to a significant decrease in 3D cultures of Cx43-EGFP MDA-MB-231 cells (f). Quantification of β -catenin expression in nuclear levels is represented by histograms for MCF-7 and MDA-MB-231 cells. Statistical analysis from three independent experiments reveals statistical significance, represented by three asterisks ($p < 0.001$) and by two asterisks ($p < 0.01$). Lamin A/C demonstrates equal protein loading, and γ -tubulin serves as a control to demonstrate lack of cytoplasmic contamination in sample preparation.

potential compared to control cells (unpublished results). As an initial insight into the tumor suppressive effects of Cx43-EGFP, full length Cx43-EGFP was noted to localize at the membrane only under culture conditions mediating a tumor suppressive effect, i.e. in 3D cultures of MDA-MB-231 cells and in 2D and 3D cultures of MCF-7 cells suggesting that the tumor suppressive effect of Cx43 may be dependent on its membranous localization and probably mediated

via its C-terminus. We have previously shown that the membranous association of Cx43 with β -catenin, α -catenin and ZO-2 is implicated in mammary epithelial cell differentiation, with β -catenin being sequestered by membranous GJ complexes away from the nucleus [19]. Given that Cx43-EGFP localized to the membrane only under culture conditions affecting the growth of MDA-MB-231 and MCF-7 cells, we asked whether over-expressed Cx43-EGFP attenuates breast

adenocarcinoma growth and invasiveness by assembling into GJ complexes that sequester β -catenin away from the nuclear compartment. Although the co-immuno-precipitation analyses does not allow for comparative quantitation of protein interactions in 2D vs. 3D cultures due to abundance of Matrigel residue in the latter, the data clearly showed that Cx43-EGFP associates with α -catenin, β -catenin and ZO-2 only in 3D cultures of MDA-MB-231 cells, as well as in 2D and 3D cultures of MCF-7 cells. Immuno-cytochemical analysis suggested that this interaction was mediated at the cell membrane as membranous co-localization between Cx43-EGFP and β -catenin was noted only in 3D cultures of MDA-MB-231 cells, and in 2D and 3D cultures of MCF-7 cells. Note that similar co-localization was observed between Cx43-EGFP and α -catenin and ZO-2 in 2D and 3D cultures of MCF-7 cells (data not shown). Several studies reported interaction of Cx with catenins and ZO proteins (reviewed by [26]). Moreover, nuclear fractionation showed that this membranous association is concomitant with a decrease in the nuclear levels of β -catenin, without affecting the total levels of β -catenin and other Cx43 associated proteins. No assessment of the cytosolic levels of β -catenin was attempted. Altogether, these findings suggest that the tumor suppressive effects of Cx43-EGFP were mediated by its assembly into GJ complexes at the membrane that sequester β -catenin away from the nucleus.

Given that β -catenin is known to regulate the expression of multiple proteins affecting cell proliferation and invasiveness [47,53,54], we set to assess whether the levels of β -catenin downstream targets such as c-myc, cyclin-D1 and p21 are decreased in conditions showing decreased nuclear β -catenin levels. Interestingly, whereas the levels of c-myc and cyclin-D1 appeared to be slightly down-regulated only in 3D cultures of MDA-MB-231 cells, a significant decrease in p21 levels was observed in 2D and 3D cultures of MCF-7 cells (data not shown). Not only do these findings serve as a functional verification of decreased nuclear β -catenin levels, but they also carry implications on the downstream effects of decreased β -catenin levels in these two cell lines. In fact, the finding that cyclin D₁ protein expression levels were decreased only in 3D cultures of MDA-MB-231 cells is in line with the cell cycle analysis data, as alterations in cyclin D₁ are known to cause a G₀/G₁ arrest and not prolongation of S-phase as noted in transfected MCF-7 cells [55]. Moreover, although decreased nuclear β -catenin levels have been shown to increase p21 expression levels [47], our findings in transfected MCF-7 cells are in line with a study proposing a tumor promoting role for p21 via its interaction with cyclin-cdk complexes [56].

All in all, our results show that Cx43-EGFP attenuates cellular growth, impedes cell cycle progression, and decreases the extravasation potential of two mammary tumor adenocarcinoma cell lines, and that context mediated proper cell-cell and cell-matrix interactions are essential for Cx43 mediated effects to be conveyed. We further report, for the first time to our knowledge, a mechanism by which Cx43 exerts tumor suppressive effects in breast cancer cells. Our data suggest that the observed phenotype was mediated via the assembly of GJ complexes with α - and β -catenins and ZO-2, and the sequestration of β -catenin from the nucleus to the membrane. The fact that the same mechanism was found occurring in two adenocarcinoma cell lines having very different molecular properties and behavior suggests that the phenotype we observed is not cell type specific. Furthermore, given that we did not assess whether GJ functionality is affected by Cx43-EGFP over-expression, we cannot rule out the possibility

of a GJIC-dependent mechanism also playing a role in one (or both) of the cell lines. However, preliminary data in our lab indicated that the overexpression of both full length and C-terminus truncated Cx43 in MCF-7 cells resulted in membranous localization of Cx43 and induced an increase in the GJIC compared to untransfected and sham transfected MCF-7 cells. Interestingly, when treating full length Cx43-GFP transfected cells with 18 α -glycerrehtinic acid (inhibitor of GJIC), there was no reversion of their decreased growth rate, thereby suggesting a GJ independent tumor suppressive role of Cx43 (data not shown).

In conclusion, we propose that Cx43 tumor suppressive effect is mediated in a context-dependent manner where GJ assembly at the membrane and the association of Cx43 with α -catenin, β -catenin and ZO-2 is possibly implicated in reducing the growth rate, invasiveness, and, hence, malignant phenotype of 2D and 3D cultures of MCF-7 cells, and only 3D cultures of MDA-MB-231 cells. This effect is probably mediated by Cx43 sequestering β -catenin at the level of the membrane and away from the nucleus. In order to provide a stronger argument on the causality of the interaction of Cx43 with β -catenin in mediating tumor suppressive effects, future studies should examine the effect of disrupting the association of Cx43 with β -catenin in normal mammary epithelial cells. The mechanism we propose would be validated further if the disruption of Cx43- β -catenin interactions in normal cells leads to their acquisition of a transformed phenotype.

Acknowledgments

This work is supported by the University Research Board and Lebanese National Council for Scientific Research; CNRS-L (RST and MES), and Medical Practice Plan (MES). Dana Bazzoun is a recipient of UNESCO-L'OREAL International Fellowship for Women in Science-2012 and the CNRS-L Award for distinguished doctoral students in 2013.

REFERENCES

- [1] Y. Liu, A. Nusrat, F.J. Schnell, T.A. Reaves, S. Walsh, et al., Human junction adhesion molecule regulates tight junction resealing in epithelia, *Journal of Cell Science* 113 (2000) 2363–2374.
- [2] D.A. Goodenough, J.A. Goliger, D.L. Paul, Connexins, connexons, and intercellular communication, *Annual Review of Biochemistry* 65 (1996) 475–502.
- [3] M. Mesnil, S. Crespin, J.L. Avanzo, M.L. Zaidan-Dagli, Defective gap junctional intercellular communication in the carcinogenic process, *Biochimica et Biophysica Acta* 1719 (2005) 125–145.
- [4] S.W. Lee, C. Tomasetto, D. Paul, K. Keyomarsi, R. Sager, Transcriptional downregulation of gap-junction proteins blocks junctional communication in human mammary tumor cell lines, *Journal of Cell Biology* 118 (1992) 1213–1221.
- [5] H. Qin, Q. Shao, H. Curtis, J. Galipeau, D.J. Belliveau, et al., Retroviral delivery of connexin genes to human breast tumor cells inhibits in vivo tumor growth by a mechanism that is independent of significant gap junctional intercellular communication, *Journal of Biological Chemistry* 277 (2002) 29132–29138.
- [6] C. Moorby, M. Patel, Dual functions for connexins: Cx43 regulates growth independently of gap junction formation, *Experimental Cell Research*, 271 (2001) 238–248.

- [7] Y.W. Zhang, M. Kaneda, I. Morita, The gap junction-independent tumoursuppressing effect of connexin 43, *Journal of Biological Chemistry* 278 (2003) 44852–44856.
- [8] J. Kalra, Q. Shao, H. Qin, T. Thomas, M.A. Alaoui-Jamali, et al., Cx26 inhibits breast MDA-MB-435 cell tumorigenic properties by a gap junctional intercellular communication-independent mechanism, *Carcinogenesis* 27 (2006) 2528–2537.
- [9] M. Momiyama, Y. Omori, Y. Ishizaki, Y. Nishikawa, T. Tokairin et al., Connexin26-mediated gap junctional communication reverses the malignant phenotype of MCF-7 breast cancer cells, *Cancer Science* 94 (2003) 501–507.
- [10] Q. Shao, H. Wang, E. McLachlan, G.I. Veitch, D.W. Laird, Down-regulation of Cx43 by retroviral delivery of small interfering RNA promotes an aggressive breast cancer cell phenotype, *Cancer Research* 65 (2005) 2705–2711.
- [11] J.X. Jiang, S. Gu, Gap junction- and hemichannel-independent actions of connexins, *Biochimica et Biophysica Acta* 1711 (2005) 208–214.
- [12] M. Kamijo, T. Haraguchi, M. Tonogi, G.Y. Yamane, The function of connexin 43 on the differentiation of rat bone marrow cells in culture, *Biomedical Research* 27 (2006) 289–295.
- [13] S. Sridharan, L. Simon, D.D. Meling, D.G. Cyr, D.E. Gutstein, et al., Proliferation of adult sertoli cells following conditional knockout of the gap junctional protein GJA1 (connexin 43) in mice, *Biology of Reproduction* 76 (2007) 804–812.
- [14] T. Yanagiya, A. Tanabe, K. Hotta, Gap-junctional communication is required for mitotic clonal expansion during adipogenesis, *Obesity* 15 (2007) 572–582.
- [15] M.E. El-Sabban, L.F. Abi-Mosleh, R.S. Talhouk, Developmental regulation of gap junctions and their role in mammary epithelial cell differentiation, *Journal of Mammary Gland Biology and Neoplasia* 8 (2003) 463–473.
- [16] R.S. Talhouk, R.C. Elble, R. Bassam, M. Daher, A. Sfeir, et al., Developmental expression patterns and regulation of connexins in the mouse mammary gland: expression of connexin30 in lactogenesis, *Cell and Tissue Research* 319 (2005) 49–59.
- [17] M.E. El-Sabban, A.J. Sfeir, M.H. Daher, N.Y. Kalaany, R.A. Bassam, et al., ECM-induced gap junctional communication enhances mammary epithelial cell differentiation, *Journal of Cell Science* 116 (2003) 3531–3541.
- [18] R.S. Talhouk, A.A. Khalil, R. Bajjani, G.J. Rahme, M.E. El-Sabban, Gap junctions mediate STAT5-independent β -casein expression in CID-9 mammary epithelial cells, *Cell Communication and Adhesion* 18 (2011) 104–116.
- [19] R.S. Talhouk, R. Mroue, M. Mokalled, L. Abi-Mosleh, R. Nehme et al., Heterocellular interaction enhances recruitment of β and α -catenins and ZO-2 into functional gap-junction complexes and induces gap junction-dependant differentiation of mammary epithelial cells, *Experimental Cell Research* 314 (2008) 3275–3291.
- [20] H. Yao, E. Ashihara, T. Maekawa, Targeting the Wnt/ β -catenin signaling pathway in human cancers, *Expert Opinion on Therapeutic Targets* 7 (2011) 873–887.
- [21] J. Sjölund, C. Manetopoulos, M.T. Stockhausen, H. Axelson, The Notch pathway in cancer: differentiation gone awry, *European Journal of Cancer* 41 (2005) 2620–2629.
- [22] J. El-Saghir, E. El-Habre, M. El-Sabban, R. Talhouk, Connexins: a junctional crossroad to breast cancer, *The International Journal of Developmental Biology* 55 (2011) 773–780.
- [23] E. McLachlan, Q. Shao, H.L. Wang, S. Langlois, D.W. Laird, Connexins act as tumor suppressors in three-dimensional mammary cell organoids by regulating differentiation and angiogenesis, *Cancer Research* 66 (2006) 9886–9894.
- [24] H.S. Lee, E.Y. Seo, N.E. Kang, W.K. Kim, Gingerol inhibits metastasis of MDA-MB-231 human breast cancer cells, *The Journal of Nutritional Biochemistry* 19 (2008) 313–319.
- [25] F.G. Giancotti, E. Ruoslahti, Integrin signaling, *Science* 285 (1999) 1028–1032.
- [26] S. Stahl, S. Weitzman, J.C. Jones, The role of laminin-5 and its receptors in mammary epithelial cell branching morphogenesis, *Journal of Cell Science* 110 (1997) 55–63.
- [27] M. Vinken, T. Vanhaecke, P. Papeleu, S. Snykers, T. Henkens, et al., Connexins and their channels in cell growth and cell death, *Cell Signal* 18 (2006) 592–600.
- [28] H.A. Dbouk, R.M. Mroue, M.E. El-Sabban, R.S. Talhouk, Connexins: a myriad of functions extending beyond assembly of gap junction channels, *Cell Communication and Signaling* 7 (2009) 4.
- [29] D. Hanahan, R.A. Weinberg, The hallmarks of cancer, *Cell* 100 (2000) 57–70.
- [30] J. Cyz, The stage-specific function of gap junctions during tumourigenesis, *Cell Mol. Biol. Lett* 13 (2008) 92–102.
- [31] C.C. Naus, J.F. Bechberger, S. Caveney, J.X. Wilson, Expression of gap junction genes in astrocytes and C6 glioma cells, *Neuroscience Letters* 126 (1991) 33–36.
- [32] L. Soroceanu, T.J. Manning, H. Sontheimer, Reduced expression of connexin-43 and functional gap junction coupling in human gliomas, *Glia* 33 (2001) 107–117.
- [33] K.K. Wilgenbus, C.J. Kirkpatrick, R. Knuechel, K. Willecke, O. Traub, Expression of Cx26, Cx32 and Cx43 gap junction proteins in normal and neoplastic human tissues, *International Journal of Cancer* 51 (1992) 522–529.
- [34] D.W. Laird, P. Fistouris, G. Batist, L. Alpert, H.T. Huynh, Carystinos GD, Alaoui-Jamali MA: Deficiency of connexin43 gap junctions is an independent marker for breast tumors, *Cancer Research* 59 (1999) 4104–4110.
- [35] S. Jamieson, J.J. Goings, R. D'arcy, D. George, Expression of gap junction proteins connexin26 and connexin43 in normal human breast and in breast tumors, *Journal of Pathology* 184 (1998) 37–43.
- [36] M.E. El-Sabban, B.U. Pauli, Adhesion-mediated gap junctional communication between lung-metastatic cancer cells and endothelium, *Invasion Metastasis* 14 (1994) 164–176.
- [37] T.J. King, P.D. Lampe, The gap junction protein connexin32 is a mouse lung tumor suppressor, *Cancer Research* 64 (2004) 7191–7196.
- [38] Y. Omori, Q. Li, Y. Nishikawa, T. Yoshioka, M. Yoshida, et al., Pathological significance of intracytoplasmic connexin proteins: implication in tumor progression, *Journal of Membrane Biology* 218 (2007) 73–77.
- [39] K. Ogawa, P. Pitchakarn, S. Suzuki, T. Chewonarin, M. Tang, et al., Silencing of connexin 43 suppresses invasion, migration and lung metastasis of rat hepatocellular carcinoma cells, *Cancer Science* 103 (2012) 860–867.
- [40] L. Kanczuga-Koda, S. Sulkowski, M. Koda, E. Skrzydlewska, M. Sulkowska, Connexin 26 correlates with Bcl-xL and Bax proteins expression in colorectal cancer, *World Journal of Gastroenterology* 11 (2005) 1544–1548.
- [41] L. Kanczuga-Koda, S. Sulkowski, J. Tomaszewski, M. Koda, M. Sulkowska, et al., Connexins 26 and 43 correlate with Bak, but not with Bcl-2 protein in breast cancer, *Oncology Reports* 14 (2005) 325–329.
- [42] K. Cusato, A. Bosco, R. Rozental, C.A. Guimaraes, B.E. Reese, et al., Gap junctions mediate bystander cell death in developing retina, *Journal of Neuroscience* 23 (2003) 6413–6422.
- [43] E. Decrock, M. Vinken, E. De Vuyst, D.V. Krysko, K. D'Herde, Vanhaecke, et al., Connexin-related signaling in cell death: to live or let die?, *Cell Death & Differentiation* 16 (2009) 524–536.
- [44] E. Gangozo, P. Ezan, J. Valle-Casuso, S. Herrero-Gonzalez, A. Koulakoff, et al., Reduced connexin43 expression correlates with c-Src activation, proliferation, and glucose uptake in reactive astrocytes after an excitotoxic insult, *Glia* 60 (2012) 2040–2049.
- [45] L. Zhan, A. Rosenberg, K. Bergami, M. Yu, Z. Xuan, et al., Deregulation of Scribble promotes mammary tumorigenesis and reveals a role for cell polarity in carcinoma, *Cell* 135 (2008) 856–878.

- [46] J.M. Burt, T.K. Nelson, A.M. Simon, J.S. Fang, Connexin 37 profoundly slows cell cycle progression in rat insulinoma cells, *Cell Physiology—American Journal of Physiology* 295 (2008) 1103–1112.
- [47] J. Kamei, T. Toyofuku, M. Hori, Negative regulation of p21 by betacatenin/TCF signaling: a novel mechanism by which cell adhesion molecules regulate cell proliferation, *Biochemical and Biophysical Research Communications* 312 (2003) 380–387.
- [48] E. Sonoda, Synchronization of cells, *Sub-Cellular Biochemistry* 40 (2006) 415–418.
- [49] J. Kota, R.R. Chivukula, K.A. O'Donnell, E.A. Wentzel, C.L. Montgomery, et al., Therapeutic microRNA delivery suppresses tumorigenesis in a murine liver cancer model, *Cell* 137 (2009) 1005–1017.
- [50] S.H. Graeber, D.F. Hulser, Connexin transfection induces invasive properties in HeLa cells, *Experimental Cell Research* 243 (1998) 142–149.
- [51] Z. Li, Z. Zhou, D.R. Welch, H.J. Donahue, Expressing connexin 43 in breast cancer cells reduces their metastasis to lungs, *Clinical and Experimental Metastasis* 25 (2008) 893–901.
- [52] W. Zhao, H.B. Han, Z.Q. Zhang, Suppression of lung cancer cell invasion and metastasis by connexin43 involves the secretion of follistatin-like 1 mediated via histone acetylation, *The International Journal of Biochemistry & Cell Biology* 43 (2011) 1459–1468.
- [53] S. Hatsell, T. Rowlands, M. Hiremath, P. Cowin, Beta-catenin and tcfs in mammary development and cancer, *Journal of Mammary Gland Biology and Neoplasia* 8 (2003) 145–158.
- [54] P. Cowin, T.M. Rowlands, S.J. Hatsell, Cadherins and catenins in breast cancer, *Current Opinion in Cell Biology* 17 (2005) 499–508.
- [55] S. Weng, M. Lauven, T. Schaefer, L. Polontochouk, R. Grover, et al., Pharmacological modification of gap junction coupling by an antiarrhythmic peptide via protein kinase C activation, *The FASEB Journal* 16 (2002) 1114–1116.
- [56] Y. Liu, F.S. Silverstein, R. Skoff, J.D. Barks, Hypoxic-ischemic oligodendroglial injury in neonatal rat brain, *Pediatric Research* 51 (2002) 25–33.